

# REPORT DOCUMENTATION PAGE

Form Approved  
OMB No. 0704-0188

Public reporting burden for this collection of information is estimated to average 1 hour per response, including the time for reviewing instructions, searching existing data sources, gathering and maintaining the data needed, and completing and reviewing this collection of information. Send comments regarding this burden estimate or any other aspect of this collection of information, including suggestions for reducing this burden to Department of Defense, Washington Headquarters Services, Directorate for Information Operations and Reports (0704-0188), 1215 Jefferson Davis Highway, Suite 1204, Arlington, VA 22202-4302. Respondents should be aware that notwithstanding any other provision of law, no person shall be subject to any penalty for failing to comply with a collection of information if it does not display a currently valid OMB control number. PLEASE DO NOT RETURN YOUR FORM TO THE ABOVE ADDRESS.

1. REPORT DATE (DD-MM-YYYY)	2. REPORT TYPE Technical Papers	3. DATES COVERED (From - To)
-----------------------------	------------------------------------	------------------------------

4. TITLE AND SUBTITLE	5a. CONTRACT NUMBER
	5b. GRANT NUMBER
	5c. PROGRAM ELEMENT NUMBER

6. AUTHOR(S) <i>Please see attached</i>	5d. PROJECT NUMBER 2302
	5e. TASK NUMBER MIG2
	5f. WORK UNIT NUMBER 346120
	8. PERFORMING ORGANIZATION REPORT

7. PERFORMING ORGANIZATION NAME(S) AND ADDRESS(ES) Air Force Research Laboratory (AFMC) AFRL/PRS 5 Pollux Drive Edwards AFB CA 93524-7048	10. SPONSOR/MONITOR'S ACRONYM(S)
---	----------------------------------

9. SPONSORING / MONITORING AGENCY NAME(S) AND ADDRESS(ES) Air Force Research Laboratory (AFMC) AFRL/PRS 5 Pollux Drive Edwards AFB CA 93524-7048	11. SPONSOR/MONITOR'S NUMBER(S) <i>Please see attached</i>
--	---

12. DISTRIBUTION / AVAILABILITY STATEMENT  
  
Approved for public release; distribution unlimited.

13. SUPPLEMENTARY NOTES

14. ABSTRACT

20030129 205

15. SUBJECT TERMS

16. SECURITY CLASSIFICATION OF:			17. LIMITATION OF ABSTRACT  A	18. NUMBER OF PAGES	19a. NAME OF RESPONSIBLE PERSON Leilani Richardson
a. REPORT Unclassified	b. ABSTRACT Unclassified	c. THIS PAGE Unclassified			19b. TELEPHONE NUMBER (include area code) (661) 275-5015

230211GS

MEMORANDUM FOR PRS (In-House Publication)

FROM: PROI (STINFO)

25 February 2002

SUBJECT: Authorization for Release of Technical Information, Control Number: **AFRL-PR-ED-TP-2002-039**  
C.T. Liu, "Investigating the Constraint Effect in a Particulate Composite Material"

**ASME 2002 Summer Meeting**  
**(Vancouver, Canada, 7-9 August 2002) (Deadline: 31 Mar 2002)**

**(Statement A)**

1. This request has been reviewed by the Foreign Disclosure Office for: a.) appropriateness of distribution statement, b.) military/national critical technology, c.) export controls or distribution restrictions, d.) appropriateness for release to a foreign nation, and e.) technical sensitivity and/or economic sensitivity.

Comments: \_\_\_\_\_  
\_\_\_\_\_  
\_\_\_\_\_

Signature \_\_\_\_\_ Date \_\_\_\_\_

2. This request has been reviewed by the Public Affairs Office for: a.) appropriateness for public release and/or b) possible higher headquarters review.

Comments: \_\_\_\_\_  
\_\_\_\_\_  
\_\_\_\_\_

Signature \_\_\_\_\_ Date \_\_\_\_\_

3. This request has been reviewed by the STINFO for: a.) changes if approved as amended, b) appropriateness of references, if applicable; and c.) format and completion of meeting clearance form if required

Comments: \_\_\_\_\_  
\_\_\_\_\_  
\_\_\_\_\_

Signature \_\_\_\_\_ Date \_\_\_\_\_

4. This request has been reviewed by PR for: a.) technical accuracy, b.) appropriateness for audience, c.) appropriateness of distribution statement, d.) technical sensitivity and economic sensitivity, e.) military/national critical technology, and f.) data rights and patentability

Comments: \_\_\_\_\_  
\_\_\_\_\_

APPROVED/APPROVED AS AMENDED/DISAPPROVED

\_\_\_\_\_  
PHILIP A. KESSEL Date  
Technical Advisor  
Space and Missile Propulsion Division

# INVESTIGATING THE CONSTRAINT EFFECT IN A PARTICULATE COMPOSITE MATERIAL

C. T. Liu  
AFRL/PRSM  
10 E. Saturn Blvd.  
Edwards AFB CA 93524-7680, U.S. A.

## ABSTRACT

In this study, the effect of constraint on the critical Mode I stress intensity factor for the onset of crack growth was investigated in a particulate composite material, containing hard particles in a rubbery matrix. Uniaxial specimens with different specimen thicknesses and initial crack lengths were tested under a constant strain rate of 8 cm/cm/min at room temperature. The tested data was analyzed and the results are discussed.

## INTRODUCTION

During the past years, considerable work has been done to study the constraint effects in metallic materials. In predicting the failure of a laboratory specimen or a full-scale structure, based on fracture mechanics theories, the constraint effect is normally referred to as the dependence of fracture toughness of materials upon specimen or structural geometries and loading conditions. Based on classical fracture mechanics theories, it is assumed that crack growth behavior in engineering materials can be characterized by a single parameter, such as the stress intensity factor or the J-integral. This assumption holds only if the local stress near the crack tip is uniquely governed by the single parameter. However, when the local stress field near the crack tip is significantly different from the J field, the concept of single parameter characterization of fracture initiation does not apply. Consequently, a two-parameter approach,  $K_I$  and T for linearly elastic materials or J and Q for elastic-plastic materials, has been proposed (1-5).

An analytical analysis of the constraint effects in elastic-plastic material was conducted by Yang, Chao, and Sutton (6-8). Using an asymptotic expansion and separation variables for the stress function, a series solution is obtained for the stress and deformation at the crack tip. For Mode I and plane strain conditions, it is shown that, when the hardening capacity of the material is high, two parameters, J and  $A_2$ , control the first three terms in the series solution; when the material exhibits less hardening, the two parameters control at least three terms. It is demonstrated that a truncated three term solution with two parameters, J and  $A_2$ , accurately characterizes the crack tip stress fields for low and high strain hardening materials, small scale yielding and large scale yielding, low and high constraint specimen geometries, and long and short cracks. The concept using J and  $A_2$  as the governing parameters is a much more rigorous and theoretically sound methodology for the prediction of onset of fracture initiation in both cleavage and ductile fracture. This statement is supported by experimental results shown in Refs 6-8. In addition, both theory and test data indicate that the constraint effect in fracture with large plasticity has opposite trend to the constraint effect in the brittle fracture with negligible plasticity. As pointed by Chao and Reuter (9) that a shallow cracked specimen would fail with a higher (lower)  $K_{Ic}$  than

a deep cracked specimen if a large scale (negligible) plastic deformation takes place at the crack tip.

In this study, the constraint effect on the critical stress intensity factor,  $K_{II}$ , for the onset of crack growth in a particulate composite material is investigated. The material investigated contains hard particles embedded in a rubbery matrix. Uniaxial specimens with different specimen thickness and initial crack lengths were tested under a constant strain rate of 8 cm/cm/min at room temperature. The tested data were analyzed and the results are discussed.

## THE EXPERIMENTS

In this study, single-edge notched tensile specimens, made from polybutadiene rubber embedded with hard particles, were used in crack propagation tests. The specimens were 2.54 cm. wide and 7.62 cm. high. Four specimen thicknesses (0.51 cm., 1.27 cm., 2.54 cm., and 3.81 cm.) and three initial crack lengths (0.508 cm., 0.762 cm., and 1.016 cm.) were considered. Prior to testing, a crack was cut at the edge of the specimen with a razor blade. The pre-cracked specimens were tested at an 8 cm/cm/min strain rate under room temperature. During the tests, a video camera was used to monitor crack growth. The raw data obtained from the tests were the crack length  $a$ ; the time,  $t$ ; and the load,  $p$ , corresponding to the measured crack length.

The recorded experimental data,  $a$ ,  $t$ , and  $p$ , were used to calculate the Mode I stress intensity factor,  $K_{II}$ . In calculating the stress intensity factor,  $K_{II}$ , for a given set of values of  $a$  and  $p$ , a nonlinear regression equation, which relates the normalized stress intensity factor,  $K_I/p$ , to the crack length,  $a$ , was used. The values of  $K_I/p$  for different crack lengths were determined from the ABAQUS computer program.

## RESULTS AND DISCUSSION

Before discussing the effects of specimen thickness and initial crack length on the Mode I stress intensity factor,  $K_{II}$ , for the onset of crack growth, we would like to first discuss the damage mechanisms near the crack tip due to the close relationship between the damage at the crack tip and the  $K_{II}$ .

It is well known that, on the microscopic scale, highly filled polymeric materials can be considered inhomogeneous materials. When these materials are stretched, the different sizes and distribution of filled particles, the different crosslink density of polymeric chains, and the variation in bond strength between the particles and the binder can produce highly nonhomogeneous local stress and strength fields. Depending on the magnitude of the local stress and the local strength, damage can be developed in the material, especially near the crack tip region. The damage developed in the material may be in the form of microvoids or microcracks in the binder or dewetting between the binder and the filler particles. Damage growth in the material may occur as material tearing or as successive nucleation and coalescence of the microcracks. These damage processes are time dependent and are the main factor responsible for the time sensitivity of strength degradation as well as the fracture behavior of the material.

A sequence of photographs showing the crack surface during the earlier stage of crack growth is shown in Fig. 1. Experimental results indicate that crack tip blunting takes place both before and

after crack growth. The material at the tip of the crack suffers very large elongation. The highly strained or damaged zones extend ahead of the crack tip, appearing as an equilateral triangle with the crack tip as its base. This damage zone is known as the failure process zone, which is a key parameter in viscoelastic fracture mechanics (10-11). When the local strain reaches a critical value, small voids are generated in the failure process zone. Due to the random nature of the microstructure, the first void is not restricted to the surface where the maximum normal strain occurs. Since the tendency for the filler particle to separate from the binder under a tri-axial loading condition is high, it is expected that voids, or a damage zone, will also be generated in the specimen's interior. Consequently, there are a large number of strands, essentially made of binder material, which separate the voids that form inside the failure process zone (Fig. 2). As the applied strain increases with time, material fracture occurs at the blunted end of the crack tip. This will always be the location of the maximum local strain. The failure of the material between the void and the crack tip causes the crack to grow into the failure process zone. This kind of crack growth mechanism continues until the main crack tip reaches the front of the failure process zone. When this occurs, the crack tip resharpen temporarily.

As mentioned earlier, the development of damage at the crack tip will redistribute the stress in the immediate neighborhood of the damaged area, resulting in an increase in stress in the material outside the damage zone. Consequently, the material outside the damage zone will also accumulate damage. The damage intensity in the newly developed damage zone depends on the magnitude of the applied load, which is a function of time. When the material inside the old failure process zone fails, a new failure process zone has formed at the tip of the resharpened crack. Experimental evidence reveals that the time required for the formation of the failure process zone decreases as the applied load is increased.

Having briefly discussed the damage mechanisms near the tip of a crack in the particulate composite material, we will proceed to discuss the experimental results on the effects of specimen thickness and initial crack length on  $K_{II}$ .

A plot of  $K_{II}$  as a function of specimen thickness for different initial crack lengths is shown in Fig. 3. From Fig. 3, it is seen that for initial crack lengths equal to 0.508 cm., 0.726 cm., and 1.016 cm., the averaged value of  $K_{II}$  is  $0.835 \text{ Mpa cm}^{0.5}$  ( $75.9 \text{ psi in}^{0.5}$ ). The variations of  $K_{II}$  among different specimen thicknesses are within the experimental scatter. Therefore, as a first approximation and for engineering applications, it can be assumed that  $K_{II}$  for the onset of crack growth is independent of specimen thickness and initial crack length, and that plane strain fracture toughness does not exist for the particulate composite material investigated in this study.

In order to obtain a fundamental understanding of the effect of damage at a crack tip on the fracture toughness, three-dimensional numerical modeling analyses were conducted, based on a linearly elastic approach. Although the geometry of the specimen analyzed in Ref. 12 was different from that of the specimen tested in this study, the trend of the effect of damage at the crack tip on  $K_{II}$  is similar and the numerical results can be used to explain the experimental phenomena observed in this study. A detailed numerical analysis can be found in Ref. 12, and only the essential and relevant part of the numerical analysis will be shown in the following paragraphs.

The specimen geometry in the finite element analysis was 20.32 by 5.08 by 1.52 cm. with a center crack of 3.8 cm long parallel to the specimen longest dimension. The specimen was divided into six layers in the thickness direction and the thickness of each layer was 0.253 cm. A uniform displacement was applied to the specimen's long edges. Due to symmetry condition, only one-eighth of the specimen was modeled and analyzed. In the analysis, a modulus of 3.45 Mpa and a Poisson's ratio of 0.4999 were used for the undamaged material. For the damaged material near the crack tip, the modulus and the Poisson's ratio were set equal to 0.414 Mpa and 0.1, respectively.

The results of three-dimensional elastic finite element analysis reveal that if there is no damage at the crack tip, the stress intensity factor,  $K_I$  varies along the crack front. The values of  $K_I$  are 1.931 Mpa cm<sup>0.5</sup> at the center of the specimen, denoted as the inner layer, 1.903 Mpa cm<sup>0.5</sup> next to the center layer, denoted as the middle layer, and 1.802 Mpa cm<sup>0.5</sup> near the surface of the specimen, denoted as the outer layer. However, when the through thickness damage occurs at the crack tip and the Poisson's ratio is equal to 0.1, the  $K_I$  values are 0.336 Mpa cm<sup>0.5</sup>, 0.339 Mpa cm<sup>0.5</sup>, and 0.342 Mpa cm<sup>0.5</sup> for the inner layer, middle layer, and outer layer, respectively. This indicates that material damage at the crack tip will result in a relatively uniform distribution of the Mode I stress intensity factor. A comparison of the numerical results with experimental observation is shown in the following paragraph.

In order to determine the shape of the crack front during crack growth, white color paint was spared into the crack. After the specimen broke, the fracture surface of the specimen was examined. It was found that the crack fronts were ideally straight, but with local irregularities. A similar phenomenon was observed by Smith and Liu (13). It is well known that for thick specimens made of metallic materials, the crack front will bow in the direction of the crack growth, creating a thumbnail shape. This suggests that there is a plane strain constraint in the center portion of the specimen, which diminishes near the side boundary. However, this is not true for the particulate composite material under investigation. Experimental data obtained in this study show that the crack front exhibited no "thumbnailing," after crack growth. The straight crack front observed in the material is believed to be due to the development of a highly damaged zone at the crack tip. The development of the highly damaged zone together with the straight crack front suggest that the transverse constraint is minimized and that a plane strain fracture toughness does not exist for this material as mentioned earlier. This indicates that, the highly filled polymeric material behaves differently from metals, and concepts that appeared clear in one instance are only found to contradict physical reality in another.

In addition to determining  $K_I$  along the crack front, the stress distributions ahead of the crack tip were also determined. Plots of thickness stress,  $\sigma_z$ , are shown in Figs.4 and 5 for the undamaged and the damaged cases, respectively. For the undamaged case, the stress state near the crack tip is tri-axial ( $\sigma_z \neq 0$ ), while at about two elements away from the crack tip the stress state changes to bi-axial ( $\sigma_z = 0$ ). Away from the crack tip, the normal stress is the dominant stress and the horizontal stress is about half of the normal stress. The stress distributions, shown in Fig. 4 for the undamaged case, suggest that the interior of the specimen is constrained, which is similar to metallic specimens. However, when the material along the crack front is damaged, it can be seen from Fig. 5 that  $\sigma_z$  is close to zero along the crack plane and the stress state becomes bi-axial. In other words, at the crack tip region, the stress state changes from plane-strain to plane-stress. The

change of the stress state is due to the redistribution of stress as a result of damage developed in the high stress region at the crack tip. The interaction of damage and stress redistribution is discussed in the following paragraph.

The damage initiation and evolution processes in a single-edge notched specimen were investigated by Liu and Kwon (14), using a micro-macro approach. It is noted that damage initiated earlier near the center than near the surface of the specimen. Since the damage state is closely related to the stress state, the difference in the damage initiation processes is due to the difference between the stress states near the center and near the surface of the specimens. It is known that near the center of the specimen, the stress state is close to the plane strain stress state as a result of relatively high constraint developed near the center of the specimen. However, near the surface of the specimen, the stress state is close to plane stress conditions. As mentioned earlier, under a tri-axial loading condition, it is relatively easy to develop microcracks in the binder and/or debond at particle-binder interface. Therefore, it is expected that damage will initiate earlier near the center of the specimen. When the material is damaged, both the stiffness and the magnitude of the stress in the damaged region will be reduced. Consequently, redistribution of the stresses occurs and the material adjacent to the damaged material will be subjected to a higher stress that, in turn, will induce damage to the material. These stress redistribution and damage evolution processes continue, and eventually all of the material in the immediate neighborhood of the crack is damaged, i.e., the thickness of the damaged material at the crack tip is equal to the thickness of the specimen. The uniform distribution of the damage along the crack front will result in a uniform distribution of stress. Since the crack growth behavior is controlled by the local stress at the crack tip, the uniform distribution of stress along the crack front will also result in a relatively straight crack front, as observed experimentally.

Referring back to Fig.5, the development of through-thickness damage at the crack tip changes the stress state from plane-strain to plane-stress. In other words, the constraint near the crack tip in the thickness direction changes from highly constrained, under the plane-strain condition, to no constraint, under the plane-stress condition. Under the plane-stress condition, it has been shown, analytically by Chao (15), that the onset of crack growth initiation is controlled by the single parameter J-integral. Numerical analyses for single-edge cracked, three-point bend, double-edge cracked, and center cracked specimens (16) reveal that the distributions of  $\sigma_{yy}$  and  $\epsilon_{yy}$  along the 0 and 45 degrees lines ahead of the crack tip fall on top of each other regardless of the loading levels (i.e., from small scale yielding to large scale yielding). This suggests that the crack tip stress fields are independent of the in-plane specimen geometry. In other words, the geometric (or constraint) effect on the crack tip stress fields is negligible. In addition to the theoretical and numerical analyses, experiments performed on very thin specimens by Deng and Wang (17) indicate that the J-integral at crack growth initiation is independent of the specimen's size and configuration. Based on the numerical and experimental analyses found in literature it can be concluded that the initial and small amount of crack growth for a fixed specimen thickness are independent of the specimen size and geometry. It is interesting to note that a similar trend has been found for the particulate composite material investigated in this study.

## CONCLUSIONS

In this study, the effects of specimen thickness and initial crack length on the critical Mode I stress intensity factor,  $K_{II}$ , were investigated. Due to the development of damage at the crack tip, the transverse, or thickness, constraint is minimized and the Poisson's effect is negligible. Consequently, a plane-stress stress state exists in the specimen. Experimental findings indicate that, on the first approximation,  $K_{II}$  is independent of specimen thickness and initial crack length for the cases considered in this study. Experimental findings also indicate that plane-strain fracture toughness does not exist for the particulate composite material under investigation.

## REFERENCES

- (1) Cardew, G.E., Goldthorpe, M.R., Howard, I.C., and Kfoury, A.P., 1984, "On the Elastic T-Term," *Fundamental of Deformation and Fracture*, pp 465-476.
- (2) Betegon, C. and Hancock J.W., 1991, "Two-parameter Characterization of Elastic-Plastic Crack -Tip Fields," *Journal of Applied Mechanics*, 58, pp 104-110.
- (3) O, Dowd, N.P. and Shih, C.F., 1991, "Family of Crack-Tip Fields Characterized by a Triaxiality Parameter-I. Structure of Fields," *Journal of Mechanics and Physics of Solids*, Vol. 39, pp.989-1015.
- (4) Anderson, T.L. and Dodds, R.H., Jr., 1991, "Specimen Size Requirements for Fracture Toughness Testing in the Transition Region," *Journal of Testing and Evaluation*, JTEVA, Vol. 19, No. 2, pp. 13-134.
- (5) Sham, T.L., 1991, "Some Evaluation of the Elastic T-Term Using Higher Order William's Functions," *International Journal of Fracture*, Vol. 48, pp.81-102.
- (6) Chao, Y.J., Yang, S., and Sutton, M.A., 1994, "On the Fracture of Solids Characterized by One or Two Parameters: Theory and Practice," *Journal of Mechanics and Physics of Solids*, Vol. 42(4), pp.629-647.
- (7) Yang, S., Chao, Y.J., and Sutton, M.A., 1993, "Higher Order Asymptotic Crack Tip Fields in a Power-Law Hardening Material," *Engineering Fracture Mechanics*, Vol.45 (1), pp.1-20.
- (8) Yang, S., Chao, Y.J., and Sutton, M.A., 1993, "Complete Theoretical Analysis for Higher Order Asymptotic Terms and the HRR Zone at a Crack Tip for Mode I and Mode II Loading of a Hardening Material," *ACTA Mechanics*, Vol. 98, pp 79-98.
- (9) Chao, Y.J. and Reuter, W.G., 1997, "Fracture of Surface Cracks," ASTM STP 1321.
- (10) Knauss, W.G., 1970 "Delayed Fracture-The Griffith Problem for Linearly Viscoelastic Materials," *International Journal of Fracture Mechanics*, Vol. 6, pp 7-15.
- (11) Schapery, R.A., 1973, "On the Theory of Crack Growth in Viscoelastic Media", Report MM- 2765-73-1, Texas A&M University.
- (12) Liu, C.T., and Ho, H., 1998, "Damage Characteristics Near Crack tip for a Particulate Composite, ASME PVP Vol. 381, Recent Advances in Solids and Structures.
- (13) Smith C.W. and Liu, C.T., 1991, "Effects of Near Tip behavior of Particulate Composite on Classical Concepts," *Journal of Composites Engineering*, Vol. 1(4), pp. 249-256.
- (14) Liu, C.T. and Kwon, Y.W., 1998, "Numerical Modeling of Damage Initiation and Evolution Processes in a Particulate Composite Material," *Modeling and Simulation Based Engineering*, Vol. 2, Editors: S.N. Atluri and P. E. O'Donoghue, Published by Tech Science



Press.

- (15) Chao, Y.J., 1993, "On the Single Parameter Controlled Fracture of Solid under Plane Stress Conditions," *International Journal of Fracture*, Vol. 62(1), R7-R10.
- (16) Liu, H.W. and Zhuang, T., 1985, "A Dual-Parameter Elastic-Plastic Fracture Criterion," *International Journal of Fracture*, Vol. 27, Nos. 3-4, pp. R87-R91.
- (17) Deng, H.W. and Wang, T., 1989, "Plane Stress Elastic-Plastic Fracture Criterion and Stress-Strain Field Around Crack Tip," *Advances in Fracture Research, ICF7*, Vol. 1, pp. 323-331.

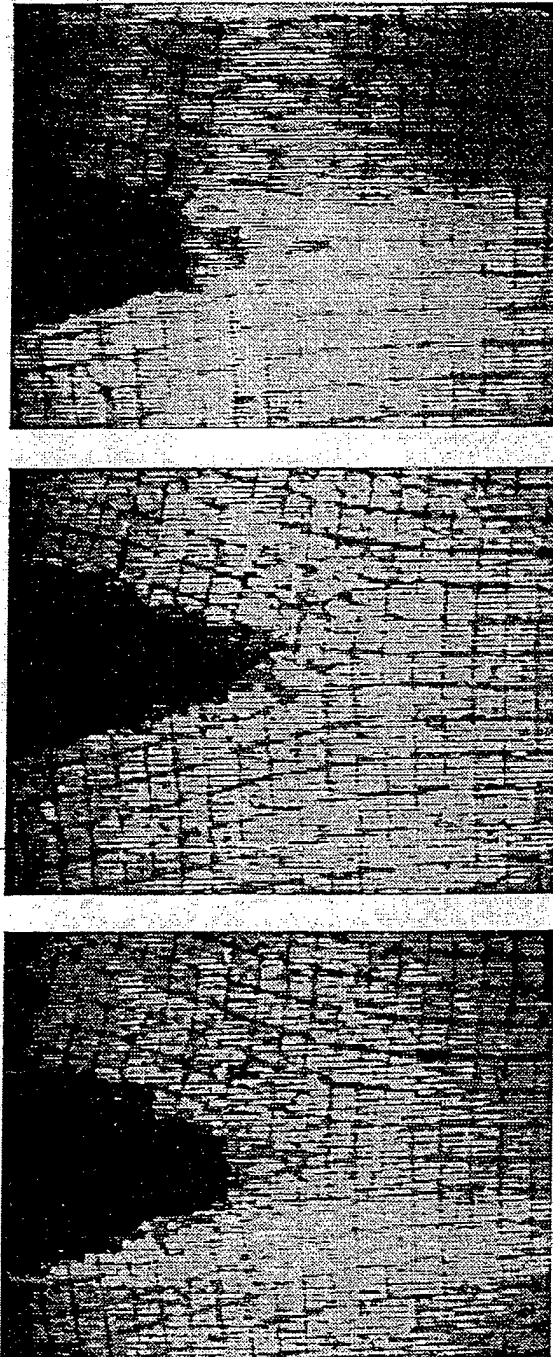


Figure 1 Crack tip profiles.

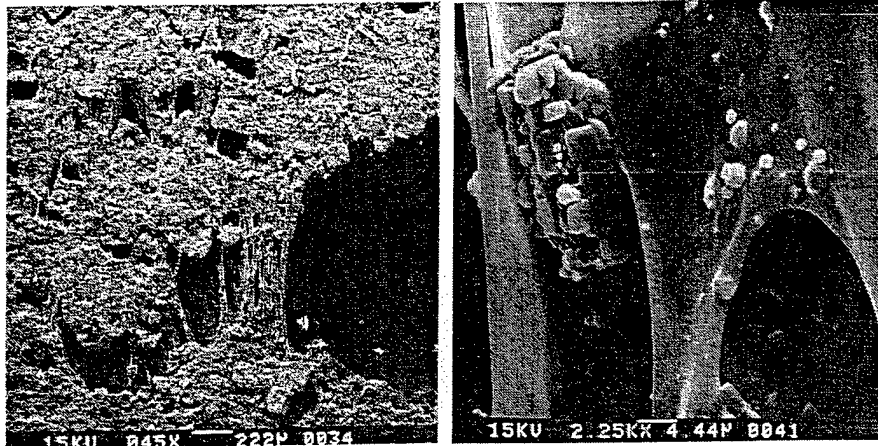


Figure 2 Failure process zone at crack tip.

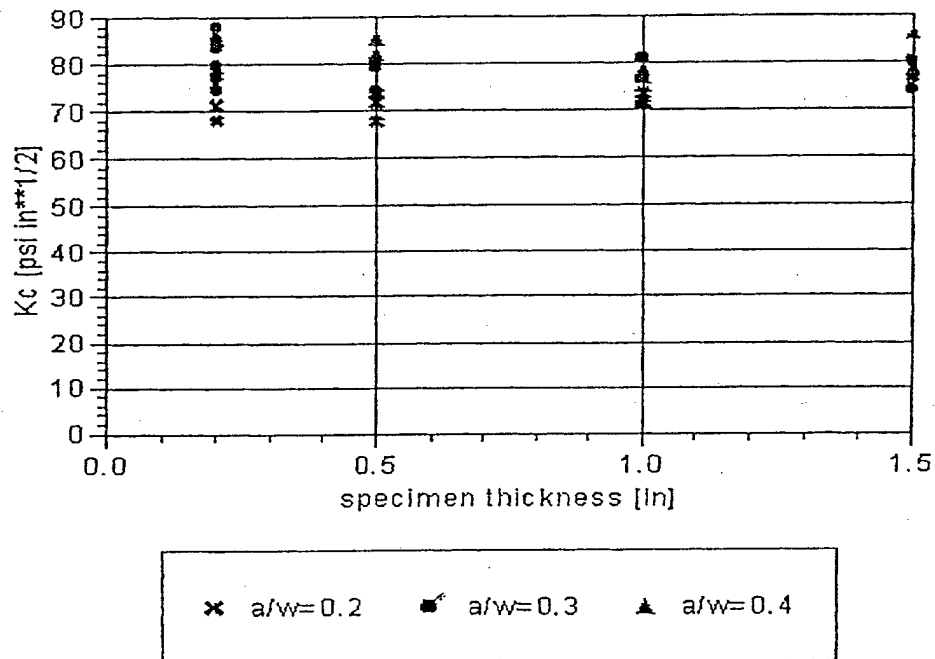


Figure 3 Critical stress intensity factors versus specimen thickness.

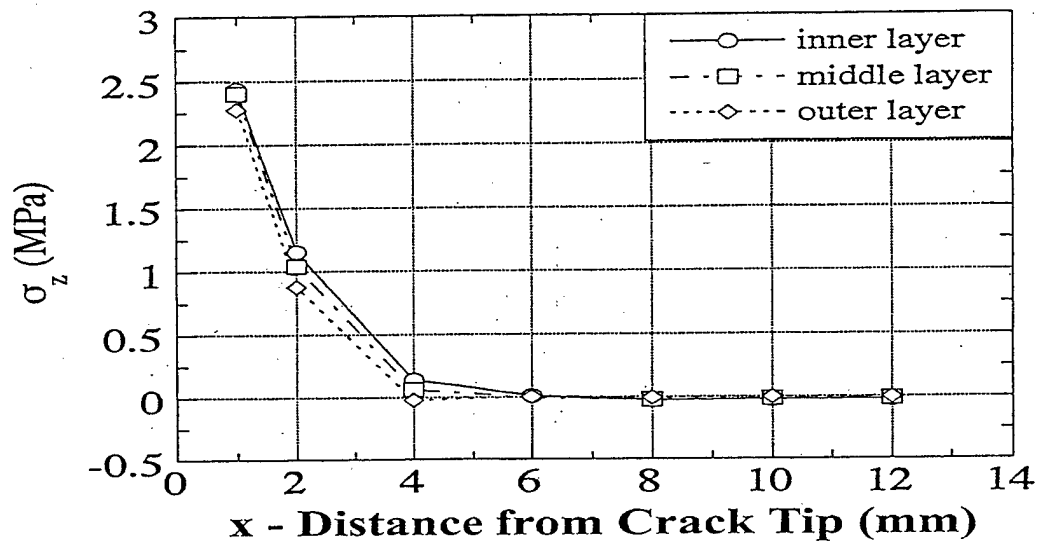


Figure 4 Distributions of thickness stress,  $\sigma_z$ , along the crack plane ( undamaged specimen)

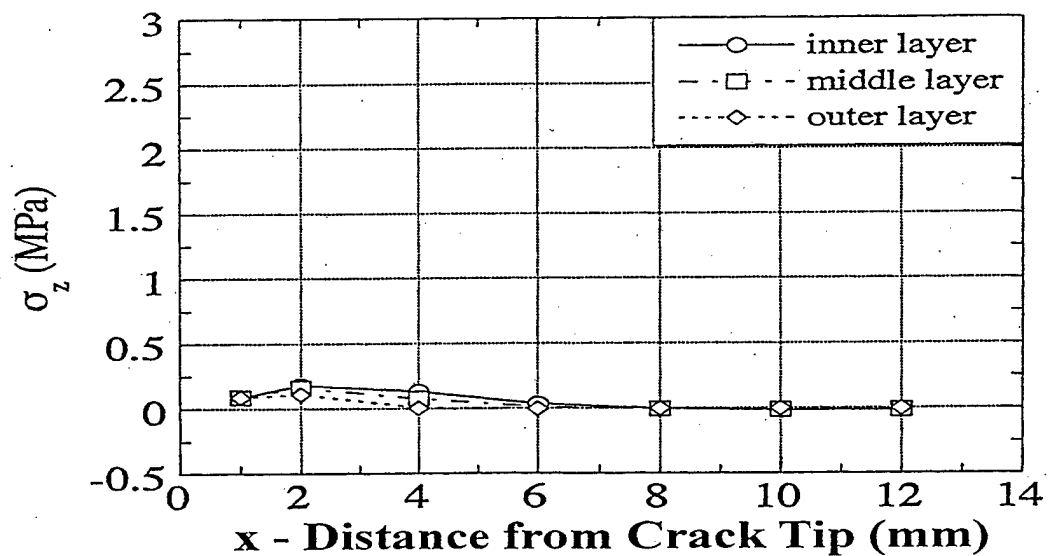


Figure 5 Distributions of thickness stress,  $\sigma_z$ , along the crack plane (damaged specimen).